

The Circumbinary Ring of KH 15D

Eugene I. Chiang & Ruth A. Murray-Clay

Center for Integrative Planetary Sciences

Astronomy Department

University of California at Berkeley

Berkeley, CA 94720, USA

`echiang@astron.berkeley.edu, rmurray@astron.berkeley.edu`

ABSTRACT

The light curves of the pre-main-sequence star KH 15D from the years 1913–2003 can be understood if the star is a member of an eccentric binary that is encircled by a vertically thin, inclined ring of dusty gas. Eclipses occur whenever the reflex motion of a star carries it behind the circumbinary ring; the eclipses occur with period equal to the binary orbital period of 48.4 days. Features of the light curve—including the amplitude of central reversals during mid-eclipse, the phase of eclipse with respect to the binary orbit phase, the level of brightness out-of-eclipse, the depth of eclipse, and the eclipse duty cycle—are all modulated on the timescale of nodal regression of the obscuring ring, in accord with the historical data. The ring has a mean radius near 3 AU and a radial width that is likely less than this value. While the inner boundary could be shepherded by the central binary, the outer boundary may require an exterior planet to confine it against viscous spreading. The ring must be vertically warped to maintain a non-zero inclination. Thermal pressure gradients and/or ring self-gravity can readily enforce rigid precession. In coming years, as the node of the ring regresses out of our line-of-sight towards the binary, the light curve from the system should cycle approximately back through its previous behavior. Near-term observations should seek to detect a mid-infrared excess from this system; we estimate the flux densities from the ring to be ~ 3 mJy at wavelengths of 10–100 μ m.

Subject headings: stars: pre-main-sequence — stars: circumstellar matter — stars: individual (KH 15D) — planetary systems — celestial mechanics

1. INTRODUCTION

The light curve of the pre-main-sequence star KH 15D, first brought to prominence by Kearns & Herbst (1998), promises to yield unique insights into the evolution of young stars

and their immediate environments. Every 48.4 days, the star undergoes an eclipse, about which we know the following:

1. Between 1995 and 2003, the eclipse duty cycle (fraction of time spent in eclipse) has grown from 30% to 45% (Hamilton et al. 2001; Winn et al. 2003).
2. During these years, ingress and egress each occupy 2–3 days out of every cycle (Herbst et al. 2002).
3. The in-eclipse light curve during these years exhibits a central reversal in brightness (Hamilton et al. 2001; Herbst et al. 2002). The amplitude of the reversal has lessened with time. In 1995, when the central reversal was first observed, the peak brightness of the reversal exceeded the out-of-eclipse brightness.
4. Light from the star in mid-eclipse is linearly polarized by a few percent across optical wavelengths, suggesting that a substantial fraction of the light in-eclipse is scattered off dust grains whose sizes exceed a few microns (Agol et al. 2004).
5. From 1967–1982, the system underwent eclipses with the same 48.4 day period as in recent years, with a duty cycle of $\sim 40\%$. In contrast to its out-of-eclipse state today, its out-of-eclipse state then was brighter by ~ 0.9 magnitudes. Moreover, the eclipse was less deep—only ~ 0.7 mag deep then as compared to today’s maximum depth of 3.5 mag. Its phase then was also shifted by ~ 0.4 relative to today (Johnson & Winn 2004).
6. From 1913–1951, no eclipse was observed (Winn et al. 2003).

We present here a physically grounded picture in which all of these observations can be understood. Its most basic elements are described in §2, where we demonstrate that the various timescales exhibited by the light curve can be explained by an inclined, vertically thin, nodally regressing ring of dusty gas that surrounds a stellar binary of which KH 15D is one member. For the ring plane to maintain a non-zero inclination with respect to the binary plane, it must be vertically warped (not merely flared; i.e., the mean inclinations of ring streamlines with respect to the binary plane must vary across the ring) so that thermal pressure gradients or ring self-gravity can offset the differential nodal precession induced by the central binary. The most natural geometry for the ring is that it be radially narrow; by analogy with narrow planetary rings that are accompanied by confining shepherds, we suggest that a planetary companion orbits exterior to the circumbinary ring of KH 15D. Perhaps the chief attraction of the model lies in its ability to make predictions; these predictions are also described in §2. A summary of our model, a discussion of the significance KH 15D carries in our overall understanding of the evolution of circumstellar, presumably protoplanetary disks, and a listing of directions for future research, are contained in §3.

2. MODEL

2.1. Basic Picture and Model Light Curves

Motivated by (1) significant radial velocity variations of KH 15D as measured by Johnson et al. (2004, submitted), (2) the observation of a central reversal in 1995 for which the peak brightness exceeded the out-of-eclipse brightness, and (3) the systematically greater brightness of the system in 1967–1982 as compared to recent years, we consider the pre-main-sequence K star KH 15D to possess an orbital companion. The data described by Johnson & Winn (2003) are consistent with a companion (hereafter, K') whose luminosity is $\sim 20\%$ greater than that of KH 15D (hereafter, K). All quantities superscripted with a prime refer to the orbital companion of KH 15D. The mass of K' should be nearly the same as that of K, and we assign each a mass of $m_b = m'_b = 0.5M_\odot$ consistent with the system's T Tauri-like spectrum. We identify the eclipse period of 48.4 days with the orbital period of the binary; for our chosen parameters, the semi-major axis of each orbit referred to the center-of-mass is $a_b = a'_b = 0.13$ AU. We assign an orbital eccentricity of $e_b = 0.5$ based on a preliminary analysis of data taken by Johnson et al. (2004). The precise value is not important; the only requirement is that the orbital eccentricity be of order unity.

The eclipses are caused by an annulus of dust-laden gas that encircles both stars, beginning at a distance $a_i > a_b$ as measured from the binary center-of-mass, and ending at an outer radius $a_f = a_i + \Delta a$. The symmetry plane of the ring is inclined with respect to the binary plane by $\bar{I} > 0$. We defer to §2.2 the issue of how such a ring maintains a non-zero \bar{I} against differential nodal precession. The ring will nodally regress at an angular speed of

$$\dot{\Omega} \sim -\bar{n} \left(\frac{a_b}{\bar{a}} \right)^2 \sim -0.13 \text{ yr}^{-1} \left(\frac{\bar{a}}{3 \text{ AU}} \right)^{-7/2}, \quad (1)$$

where \bar{a} is the mean radius of the ring and \bar{n} is the mean motion evaluated at that radius. Equation (1), derived from standard celestial mechanics perturbation theory, is only accurate to order-of-magnitude, since it relies on an expansion that is only valid to first order in m'_b/m_b . Nonetheless, it is sufficiently accurate to establish the reasonableness of our picture in the context of the observations; corrections will not alter our conclusions qualitatively.

As illustrated in Figure 1, eclipses occur whenever the ascending or descending node of the ring regresses into our line-of-sight towards the stellar binary. The observer is assumed to view the binary orbit edge-on, or nearly so. The orbital motion of a given star about the center-of-mass causes the star to be occulted by varying columns of ring material. Eclipses occur with a period equal to the binary orbital period. The shape of the eclipse—e.g., the presence or absence of central reversals, or the level of brightness out-of-eclipse—is modulated

over the longer timescale of nodal regression.

Figure 2 depicts schematically and in more detail some of the ring-binary geometries that are possible. Each panel in Figure 2 is marked with a letter corresponding to a particular longitude of ascending node, Ω , of the ring on the binary plane; the letters in Figures 1 and 2 correspond to the same geometries. For example, in panel B of Figure 2, when the edge of the ring occults the apoapsis of the orbit of K' , the observer should see eclipses like those witnessed in 1967–1982; star K is always seen, while star K' periodically disappears behind the ring; out-of-eclipse, light from two stars is seen, while in mid-eclipse, only one star is seen. In panel C, as the ring’s edge regresses further inwards to just cover the binary center-of-mass, only the periapsis of K' and the apoapsis of K remain unobscured; during the eclipse of K , the brighter companion K' emerges briefly, producing a central reversal like that seen in 1995. Other panels in Figure 2 correspond to other longitudes of the node, and can be identified with other observed behaviors of the light curve. In particular, the regression of the ring’s edge onto and past the periapsis of K' (panel D) results in a concomitant weakening of the central reversal and a lengthening of the duration of the eclipse of K —trends seen today.

A key parameter of the ring is its vertical scale height, which must be small enough to yield short ingress and egress times, but large enough to cover substantial fractions of the binary orbit. We model the ring with a Gaussian atmosphere perpendicular to its midplane at a given radius, as befits material with constant vertical velocity dispersion. We describe the absorption coefficient (units of inverse length) by

$$\alpha = \alpha_i \left(\frac{a}{a_i} \right)^{-\Gamma} \exp\{-[\theta(a)/\theta_0]^2\}, \quad (2)$$

where $\theta(a)$ is the latitudinal angle measured from the *local* ring plane at disk radius a , and θ_0 , α_i and Γ are constants. We prescribe a power law for the inclination of the local ring plane with respect to the binary plane:

$$I(a) = I_i \left(\frac{a}{a_i} \right)^\beta, \quad (3)$$

where I_i and β are constants. The function $I(a)$ specifies the vertical *warp* across the ring, as distinct from the finite thickness described by the Gaussian in equation (2).¹ A warp must be present to maintain rigid nodal precession; see section §2.2. Our standard choices for

¹A warp is not the same as a flare. The latter term refers to an increasing θ_0 with disk radius a .

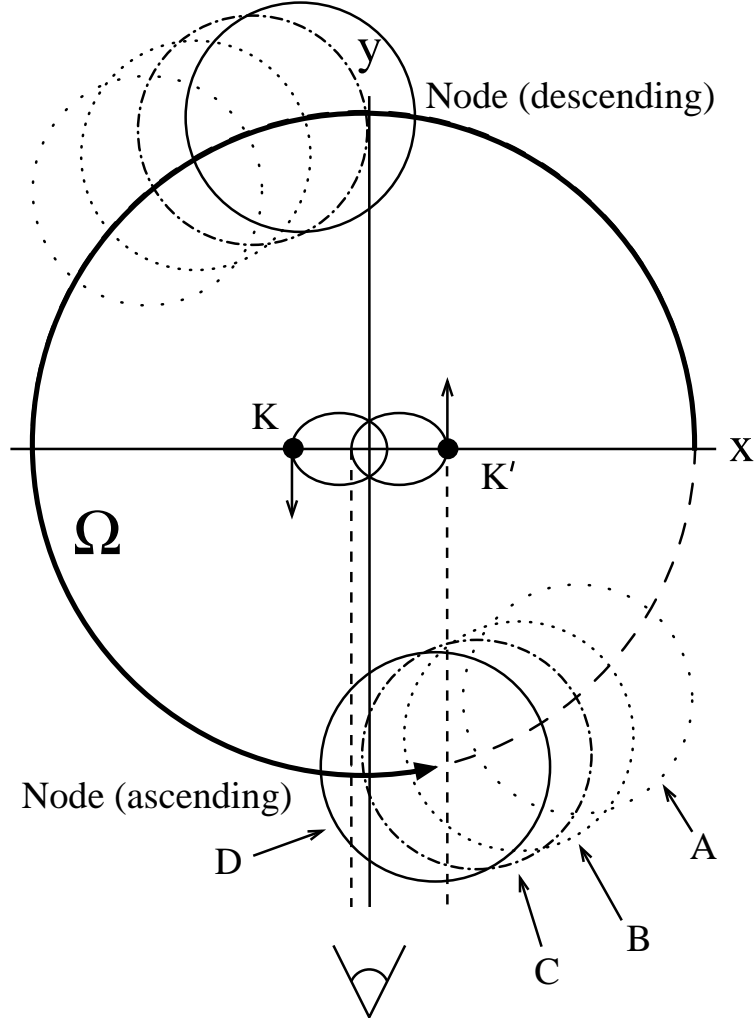


Fig. 1.— Schematic of the KH 15D system (not to scale). The star KH 15D is denoted K, while its orbital companion is denoted K'. The two stars are of nearly the same mass and occupy highly eccentric orbits. Surrounding the binary is a dusty ring, whose ascending and descending nodes (“footprints”) on the binary plane are indicated by smaller circles. The sizes of the circles represent the amount of obscuring material viewed along our line-of-sight in the binary plane; the sizes are set by the ring’s inner and outer radii, the degree of vertical flaring, and the inclination profile (mean inclination plus warp). The quadrupole field of the central binary causes the ascending node of the ring to regress (travel counter to the direction of orbital mean motion) from position A to position D. The longitude of ascending node is measured counter-clockwise from the x-axis and is denoted by Ω . The observer views the binary orbit edge-on from below. More detailed schematics of the ring-binary geometry corresponding to phases A–D can be found in Figure 2.

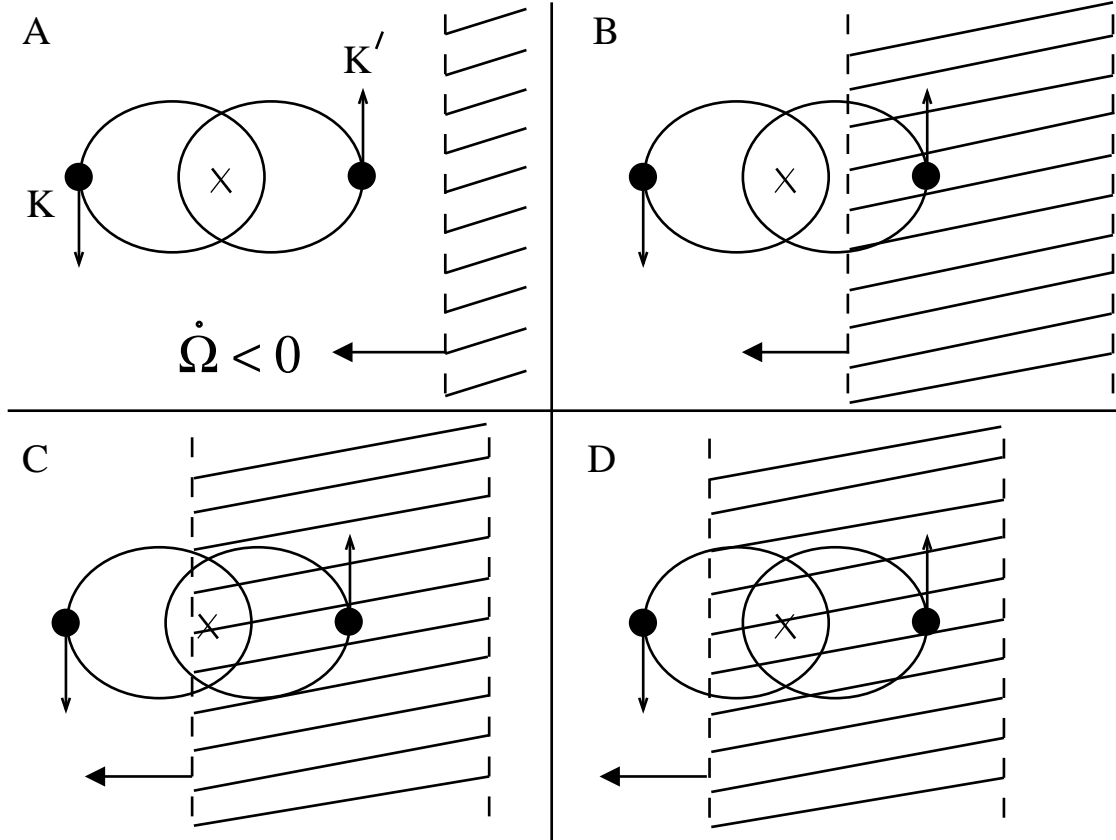


Fig. 2.— Schematic of relative ring-binary geometries. The inset letters in each panel correspond to the same geometries depicted in Figure 1; the observer views the binary from the bottom of the page. In panel A, no eclipses occur, consistent with the historical data prior to 1951. In panel B, the ring's node has regressed to block the apoapsis of star K'; eclipses like those seen from 1967–1982 should be seen. In panel C, eclipses like those seen from 1995–2000 should be evident, with central reversals of brightness during mid-eclipse when star K' emerges at its periapsis. In panel D, the node covers the entire orbit of K' and an increasingly large fraction of the orbit of K; central reversals should be much weaker, and the eclipse duty cycle greater, than in C. While we have drawn the occulted region as a hatched region of definite area, the intervening optical depth along different rays is a smooth function, both in reality and in our computations of the light curve.

model parameters are contained in Table 1. These are chosen to reproduce approximately the observed light curves, as we describe below.

Computation of the light curve in the absence of scattering is a straightforward exercise in numerical integration. For simplicity, and because our purpose here is to introduce new ideas, we model the stars as point sources. Light from each star is extinguished as $\exp(-\int \alpha dl)$, where the integral is performed along a ray from the star to the observer. The orientation of the observer is fixed such that the binary orbit is viewed edge-on and the velocity of K at its apoapsis is directed towards the observer; see Figure 1.

Figure 3 displays a sequence of light curves for parameters corresponding to model 1 in Table 1. Each panel corresponds to a particular choice of Ω ; this angle decreases from $\Omega = 282^\circ$ to $\Omega = 259^\circ$ from top left to bottom right. Four panels are labelled with letters according to the same scheme used in previous figures. We assign the year 1995.0 to panel C, in which the peak brightness of the central reversal exceeds the out-of-eclipse brightness. Dates for all other panels are computed according to equation (1).

We are encouraged by the agreement between Figure 3 and the observations as summarized in §1. A primary shortcoming of our computations is the neglect of starlight scattered off the circumbinary ring and potential other material, such as a remnant envelope. It is our hope that scattered light sets a lower limit to the observed flux, ~ 3.5 magnitudes below the magnitude of K, as suggested by Agol et al. (2003). We indicate such a floor by the lower dashed line in every panel of Figure 3.

Predictions for the light curve for a given set of model parameters are readily computed. In the near future, the system should simply cycle backwards through its previously observed behavior, as the trailing edge of the node sweeps across the binary orbit.² The evolution will not, however, be exactly mirror-symmetric; for example, in later years, we do not expect the central reversal to exceed the out-of-eclipse brightness, since K is less luminous than K'; compare, in Figure 3, the bottom left panel to panel C. Changes in viewing orientation will also alter details.

We defer to modellers of more sophistication than ourselves the task of rigorously fitting the observed light curves to achieve predictions of greater robustness. None of the parameters in Table 1 should be considered unique; for example, we generated light curves similar to those shown in Figure 3 by reducing I_i and θ_0 simultaneously by factors of 10.

²If the observer views the binary orbit exactly edge-on as shown in Figure 1, it is unclear from the light curve whether the ascending or descending node is occulting the binary. The degeneracy can be broken for other viewing geometries.

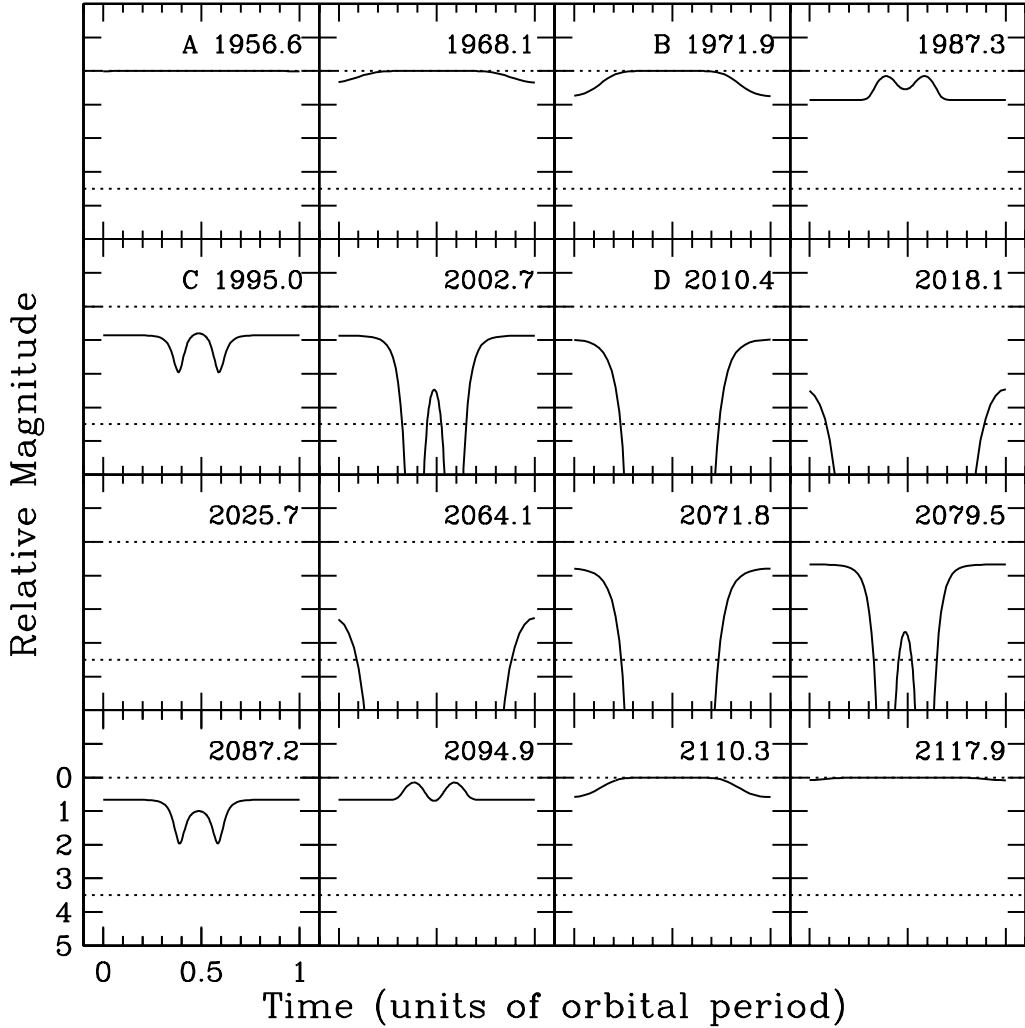


Fig. 3.— Computed light curves for the KH 15D system, using parameters listed under model 1 of Table 1. Inset letters A–D refer to the same geometries illustrated in Figures 1 and 2. The inset number refers to the year in which behavior similar to that computed was actually observed; after we assign the year 1995.0 to panel C in which the strongest central flash is evident, years for all other panels are computed according to the nodal regression rate [equation (1)] and the value of Ω appropriate to a given panel. The upper dashed line in each panel indicates the maximum system brightness; the lower dashed line indicates a possible minimum system brightness established by light scattered off circumbinary material. Predictions for future years are shown; roughly speaking, the system should cycle through its previous behavior in reverse order.

We turn now to two related theoretical issues: the ability of the ring to maintain a non-zero inclination, and the determination of its inner and outer radii.

2.2. Maintaining a Non-Zero Inclination

In the absence of thermal pressure and ring self-gravity, a circumbinary disk of particles, initially inclined with respect to the binary plane and characterized by the same longitude of ascending node over all radii, would precess differentially; radial variations in the nodal precession rate due to the quadrupole field of the central binary would reduce the mean inclination of the disk to zero. Narrow planetary rings that are observed to maintain non-zero inclinations with respect to the equator planes of their host planets avoid this fate by virtue of their self-gravity, with some modification by pressure gradients (Chiang & Culter 2004; Chiang & Goldreich 2000; Borderies, Goldreich & Tremaine 1983). Gaseous disks can also maintain rigid precession by the action of thermal pressure (Papaloizou & Pringle 1983; Papaloizou & Lin 1995; Larwood & Papaloizou 1997; Lubow & Ogilvie 2000; Lubow & Ogilvie 2001) and/or self-gravity; some indirect evidence for rigid precession in gaseous, circumprimary disks is available from X-ray binaries (Larwood 1998) and pre-main-sequence binaries (Terquem et al. 1999).

Whether the ring is composed of particles or gas, it must be vertically warped so that either pressure or self-gravity exerts forces normal to the local ring plane. That is, given a ring in which each streamline has the same longitude of ascending node as every other streamline, there must exist a gradient in inclination across the ring.

Unlike the case of planetary rings, thermal pressure alone is sufficient to offset differential precession in gaseous, circumstellar disks because the gas sound speed, c_s , is typically a healthy fraction of the Kepler orbital speed, $\bar{n}\bar{a}$. To maintain rigid precession across a circumbinary ring of radial width $\Delta a < \bar{a}$ by gas pressure alone, the ring must exhibit a fractional variation in inclination of order

$$\frac{\Delta I}{I} \sim -0.1 \left(\frac{\bar{n}\bar{a}/c_s}{20} \right)^2 \left(\frac{a_b/\bar{a}}{0.05} \right)^2 \left(\frac{\Delta a/\bar{a}}{0.5} \right)^3, \quad (4)$$

where the numerical evaluation is appropriate for parameters listed under model 1 of Table 1. The narrower the ring, the less severe is the requisite warp. The inclination gradient is negative; from its inner edge to its outer edge, the ring tends to bend back down towards the binary plane. This order-of-magnitude expression can be derived by setting the differential precession rate between two infinitesimally narrow wires due to the quadrupole field of the

central binary equal to the differential precession rate due to the repulsive pressure between the wires; the spirit of the calculation is the same as can be found in Goldreich & Tremaine [1979a, see their equations (12)–(14); or 1979b]. Equation (4) must be viewed with caution; it neglects pressure forces at ring boundaries that could be important, especially if the pressure changes over lengthscales that are shorter than Δa (such as the vertical scale height h ; see Chiang & Goldreich 2000). It also assumes zero radial gas flow between disk annuli; Lubow & Ogilvie (2004, personal communication) have shown that by accounting for the near-resonant forcing of radial velocities by gas pressure (Papaloizou & Pringle 1983; Papaloizou & Lin 1995), the magnitude of the warp might be reduced from that predicted by equation (4). Definitive models of the ring will require these issues to be addressed; for now, we feel these concerns will not alter our qualitative conclusions.

If rigid precession is maintained by self-gravity alone, the magnitude of the warp is a function of the ring mass, m_r :

$$\frac{\Delta I}{\bar{I}} \sim 0.1 \left(\frac{m'_b/m_r}{500} \right) \left(\frac{a_b/\bar{a}}{0.05} \right)^2 \left(\frac{\Delta a/\bar{a}}{0.5} \right)^3, \quad (5)$$

where the numerical evaluation is appropriate for the parameters listed under model 2 of Table 1. Here the inclination gradient is positive. The same steep dependence on ring width is evident. Our chosen ring mass, equal to the mass of Jupiter, is comparable to that expected from the minimum-mass solar nebula and still yields a ring that is gravitationally stable in the Toomre Q sense; the ring mass divided by the central mass must approach $c_s/\bar{n}\bar{a} \sim 1/20$ before gravitational instability in the gas becomes relevant.

If $m_r/m'_b \ll 1/500$, then equation (4) better describes the warp, to the extent that it is difficult to imagine values for c_s much different from that assumed. If $m_r/m'_b \gg 1/500$, then equation (5) better describes the warp.

Models 1 and 2 are intended to represent disks for which thermal pressure and self-gravity, respectively, are wholly responsible for maintaining a non-zero \bar{I} . In model 1, the inclination of a streamline decreases from $I(a_i) = 20^\circ$ to $I(a_f) = 10^\circ$; in model 2, $I(a_i) = 10^\circ$ and $I(a_f) = 20^\circ$. The inclination profiles so prescribed accord with equations (4) and (5). Light curves from model 1 are displayed in Figure 3, while those from model 2 are showcased in Figure 4. We consider the agreement with the observations to be comparable between the two cases. Note that for model 2, the binary orbit is less severely occulted, in contrast to model 1. Moreover, the ingress and egress profiles are sharper in model 2.

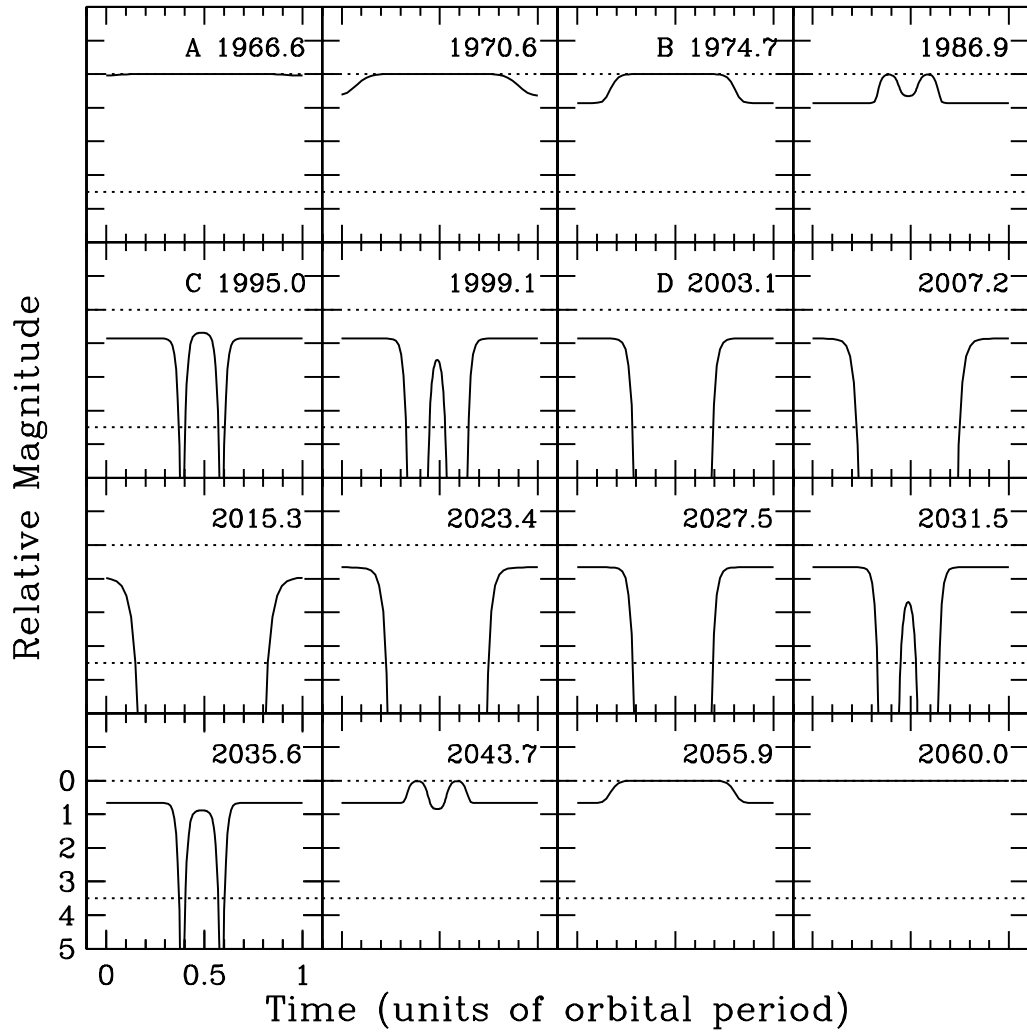


Fig. 4.— Same as Figure 3, but for model 2, for which the inclination gradient across the ring is positive. The evolution of light curves is qualitatively the same as that for model 1, for which the inclination gradient is negative.

2.3. Radial Boundaries

2.3.1. The Outer Boundary

If this dusty disk extends too far outwards in the radial direction ($\Delta a \gg a_i$), at least two problems arise: (1) how to maintain rigid precession across an extended disk, and (2) how to prevent a disk of large vertical thickness from occulting the central binary completely at all times. We discuss each of these in turn.

“Rigid tilt modes” can be described for disks that extend for more than one decade in radius (Lubow & Ogilvie 2004, personal communication). Gas pressure can enforce such a mode over a length travelled by a sound wave in a differential precession time (~ 20 AU for a sound speed of ~ 1 km s $^{-1}$ and a differential precession time of $\sim 10^2$ yr evaluated at 3 AU). Self-gravity could extend this length. It is unclear why such a mode would dominate a large, extended disk; on the other hand, while it is similarly not understood why narrow planetary rings exhibit rigid tilts, at least clear observational evidence exists that they do (French et al. 1991).

The second problem could be avoided if the ring is sufficiently thin and sufficiently warped that material is bent out of the line-of-sight. Dust need not be well-mixed with gas; the tidal force of stellar gravity can pull grains towards the local disk midplane. Evidence for dust settling is abundant in classical T Tauri and Herbig Ae systems [see, e.g., Chiang et al. (2001)], but the required degree of settling becomes more severe with increasing disk radius.³

While the above problems can be surmounted to varying degrees, we still feel drawn to a radially narrow ring of dust as the most natural solution. Our assumptions regarding the central stellar binary, together with the requirement that the ring’s nodal precession rate accord with the observed history of light curves, set the mean radius of the ring to be $\bar{a} \approx 3$ AU. Having experimented with a variety of model parameters, we feel no more precise statement can be made other than that $\Delta a \lesssim \bar{a}$.

What could be responsible for such a ring’s confinement at its outer radius? Perhaps the most obvious proposal to make is to draw an analogy with narrow planetary rings that are radially confined by shepherd moons (see, e.g., Goldreich & Tremaine 1982). These rings

³The opening angle of $\theta_0 \sim 0.3$ deg that we employ in models 1 and 2 for the dust disk is an order of magnitude lower than the typically assumed opening angle of the gas disk at this radius. This low value, presumably the result of dust settling, still sits an order of magnitude above the minimum opening angle set by Richardson turbulence.

successfully maintain non-zero inclinations with respect to the equator planes of their central planets. Unfortunately, mass estimates for shepherding planets in the case of KH 15D cannot be made without knowing the viscosity of disk material; the viscosity could easily be so tiny that planets less massive than Jupiter could confine the ring against viscous spreading.

An alternative to confinement by a planetary companion could be provided by radial migration of dust due to aerodynamic drag (for the background physics, see, e.g., Youdin & Shu 2002; Youdin & Chiang 2004; and references therein). In this picture, dust accretes relative to gas towards the inner edge of the disk, leaving behind dust-depleted gas. The accretion rate depends on grain size, however, and it seems implausible to expect a grain size distribution that is so narrowly peaked in a given size range that the disk nearly completely empties itself of radial optical depth outside $a \sim a_i$.

2.3.2. *The Inner Boundary*

The central stellar binary itself could shepherd the inner edge of the ring. Artymowicz & Lubow (1994) compute $a_i/a_b \approx 5$ for the case of binaries having $e_b \approx 0.5$ and $m'_b/m_b \approx 0.3$, and moderately viscous disks. This would place $a_i \approx 0.6$ AU. The true value for the case of KH 15D would be greater than this since the binary mass ratio is closer to unity.

An AU-sized inner hole can naturally explain the observed absence of near-infrared excess for KH 15D. Such excesses arise from reprocessing of starlight by and/or active accretion of disk material at stellocentric distances inside a few AU. By carving out an AU-sized inner hole in the disk surrounding the T Tauri star TW Hydra, Calvet et al. (2002) succeed in reproducing the observed deficit of near-infrared emission in its spectral energy distribution. For TW Hydra, disk material at stellocentric distances greater than an AU produces excess emission at wavelengths longward of 10 microns (see also Weinberger et al. 2002). We hold the same expectation for KH 15D, as described quantitatively in the next section.

3. SUMMARY AND DISCUSSION

We have proposed that the light curves of the pre-main-sequence star KH 15D can be understood if that star harbors a companion of slightly greater luminosity and nearly identical mass, on an orbit having eccentricity of order unity. Today, this companion is occulted by a circumbinary ring of dusty gas. To cover one star and not the other, the ring is necessarily inclined with respect to the binary plane; to maintain uniform nodal precession

and a mean inclination, it is also necessarily warped.⁴ Thermal pressure gradients or self-gravity readily furnish the forces necessary to maintain rigid precession; the inclination gradient across the ring is negative or positive depending on whether pressure or gravity dominates. While a variety of ring geometries appear to give fits of comparable quality to the light curves, the following dimensions to the ring seem difficult to avoid: a mean radius of $\bar{a} \approx 3$ AU, and a radial width $\Delta a \lesssim \bar{a}$. Modelling the scattered optical light from the system will yield constraints on the ring geometry that we have been unable to provide.

Looking farther ahead, we should expect an observable mid-infrared excess from this ring by passive reprocessing of starlight. To our knowledge, no mid-infrared observation has been taken of KH 15D. At wavelengths of 10–100 μm , we estimate flux densities of $F_\nu \sim 3$ mJy for the ring parameters in Table 1, well above stellar photospheric flux densities. This emission arises largely from the optically thin surface layers of the disk that are directly exposed to central starlight (Chiang & Goldreich 1997). A crudely estimated spectral energy distribution is displayed in Figure 5. At wavelengths longer than \sim 100 microns, the flux density should decrease, if, as we suspect, the ring is truncated at an outer radius of a few AUs. In making this estimate, we assume that only 10% of full flux from a face-on, optically thick disk interior is observed because of a nearly edge-on viewing orientation and that the angle with which starlight grazes the surface of the warped dust disk is $\Delta I \sim 1^\circ$ (see, e.g., Chiang & Goldreich 1997, 1999).

Observations of the stars in and out of eclipse at longer wavelengths would enable us to measure the wavelength dependence of dust opacity and thereby constrain the size distribution of disk grains. Such occultation observations are routinely performed for planetary rings from ultraviolet to radio wavelengths, and have provided a wealth of information for such systems. Non-thermal radio emission from T Tauri stars might well be strong enough to provide a background light source.

The period of eclipses is that of the binary orbital period, while the shape of the light curve is modulated over the much longer timescale of nodal precession. We anticipate that in the coming decades, as the ring node regresses past the binary orbit, the eclipses will eventually repeat their prior behavior in reverse order: the eclipses will narrow, the central flashes will amplify, there will be a shift in eclipse phase by 0.5, and eventually the eclipses will cease altogether (until the other node swings by, centuries hence). The fraction of time during which the circumbinary ring (either its ascending or descending node) occults either star is roughly $40^\circ/360^\circ \sim 11\%$.

⁴The ring is likely to be eccentric as well, with a mean eccentricity induced by secular forcing from the binary.

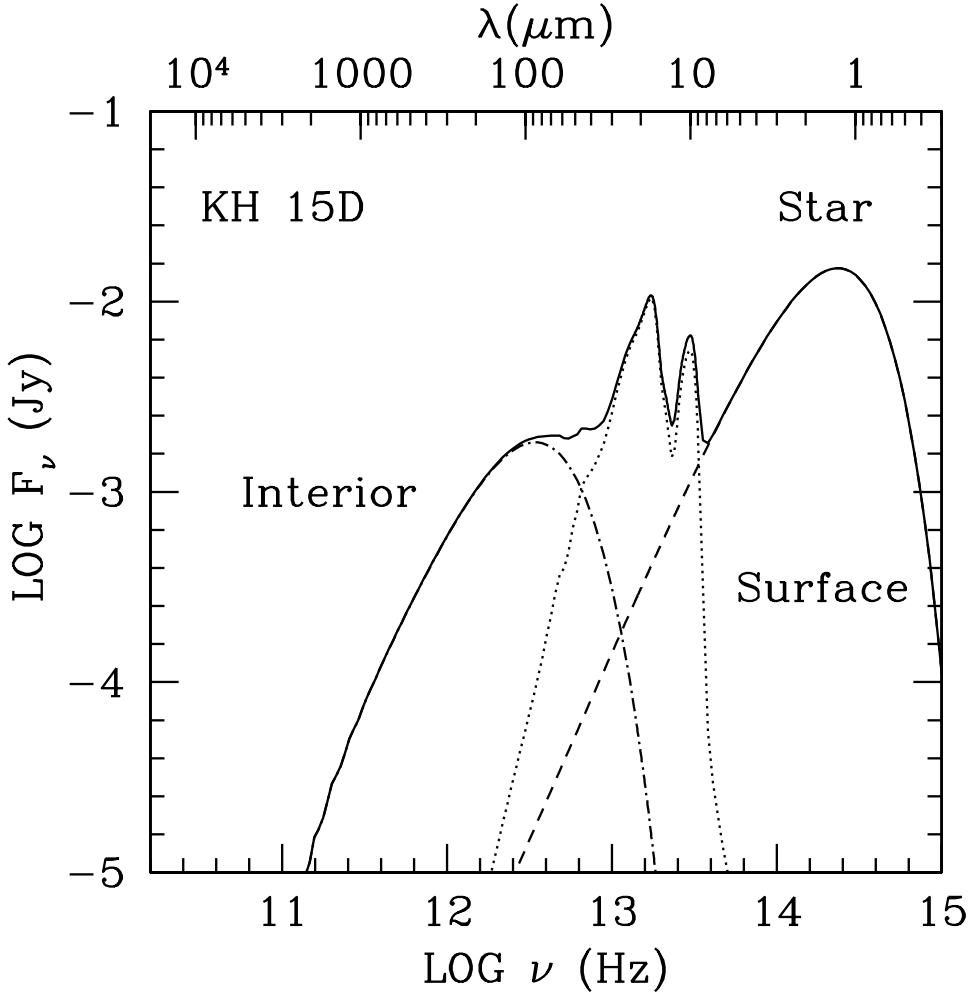


Fig. 5.— Predicted flux density of thermal emission from the KH 15D system, crudely estimated using the formalism of Chiang et al. (2001, hereafter C01). Only emission from one star is shown, though both stars are accounted for in calculating the reprocessed flux from the ring. Disk parameters are the same as those of the standard model of C01 except for the inner radius ($a_i = 1$ AU), the outer radius ($a_o = 5$ AU), and the height of the photosphere relative to the gas scale height ($H/h = 1.4$). Our choice of H/h simulates a ring warp for which $\Delta I = 1^\circ$. To account for the nearly edge-on viewing geometry, the flux from the disk interior has been reduced from the face-on value by a geometric projection factor of 10. The flux from the optically thin disk surface has not been adjusted from its face-on value (see Chiang & Goldreich 1999).

The framework we have presented can easily accommodate fine details of the light curve. For example, slight differences between ingress and egress time intervals (Herbst et al. 2002) can be reproduced by orienting the observer at a small angle relative to quadrature of the binary orbit, thereby taking advantage of the non-uniform angular motion of a star.

Once the ring’s node regresses past the orbit of the companion of KH 15D over the next few decades, the spectrum of the star can be cleanly obtained. Measurement of the masses and luminosities of both components of this pre-main-sequence binary would provide an important test of evolutionary tracks on Hertzsprung-Russell diagrams.

The requirement of a radially narrow ring suggests confinement by tidal torques. The central binary could provide the torque required to prevent viscous spreading of the inner edge at $a_i \sim 1$ AU. Shepherding the outer edge a few AUs away would require a circumbinary planet. If this picture is correct, then the epoch of planet formation could not have lasted more than the age of this T Tauri star, a few million years (Sung, Bessel, & Lee 1997).

Many thanks to John Johnson and Geoff Marcy for generously sharing their preliminary radial velocity results with us. We are grateful to Steve Lubow and Gordon Ogilvie for broadening discussions, Drake Deming for motivating us to calculate the thermal emission from the ring, Eric Ford for preliminary calculations of scattered light, and an anonymous referee for improving the presentation of this paper. E.I.C. acknowledges support by National Science Foundation Planetary Astronomy Grant AST 02-05892 and Hubble Space Telescope Theory Grant HST-AR-09514.01-A.

Table 1. Model Ring Parameters^a

Parameter	Model 1 ^b	Model 2 ^c
\bar{a} (AU)	3	2.5
Δa (AU)	1.50	1.00
α_i (AU ⁻¹) ^d	50000	50000
Γ	4.0	4.0
θ_0 (deg)	0.30	0.35
I_i (deg)	20	10
β	-2.0	1.7

^aNone of the parameters in this table should be regarded as uniquely fitting the circumbinary ring of KH 15D; our only secure conclusions are that $\bar{a} \approx 3$ AU and $\Delta a \lesssim 3$ AU; see text.

^bModel 1 represents a disk whose non-zero inclination is maintained by thermal pressure; the warp index β is negative so that the ring tilts increasingly towards the binary plane from small to large radius.

^cModel 2 represents a disk whose non-zero inclination is maintained by self-gravity; the warp index β is positive so that the ring tilts increasingly away from the binary plane from small to large radius.

^dA value of $\alpha_i = 50000/\text{AU}$ is consistent with an opacity of

$1 \text{ cm}^2 / (\text{g of gas})$ and a midplane gas density of $3 \times 10^{-9} \text{ g/cm}^3$.

REFERENCES

Agol, E., Barth, A.J., Wolf, S., & Charbonneau, D. 2004, *ApJ*, 600, 781

Artymowicz, P., & Lubow, S.H. 1994, *ApJ*, 421, 651

Borderies, N., Goldreich, P., & Tremaine, S. 1983, *AJ*, 88, 226

Calvet, N., et al. 2002, *ApJ*, 568, 1008

Chiang, E.I., & Culter, C.J. 2003, *ApJ*, 599, 675

Chiang, E.I., & Goldreich, P. 1997, *ApJ*, 490, 368

Chiang, E.I., & Goldreich, P. 2000, *ApJ*, 540, 1084

Chiang, E.I., et al. 2001, *ApJ*, 547, 1077

French, R.G., Nicholson, P.D., Porco, C.C., & Marouf, E.A. 1991, in *Uranus*, ed. J.T. Bergstrahl, E.D. Miner, & M.S. Matthews (University of Arizona Press), 327

Goldreich, P., & Tremaine, S. 1979a, *Nature*, 277, 97

Goldreich, P., & Tremaine, S. 1979b, *AJ*, 84, 1638

Goldreich, P., & Tremaine, S. 1982, *ARA&A*, 20, 249

Herbst, W., et al. 2002, *PASP*, 114, 1167

Hamilton, C.M., Herbst, W., Shih, C., & Ferro, A.J. 2001, *ApJ*, 554, L201

Johnson, J.A., & Winn, J.N. 2004, *AJ*, 127, 2344

Johnson, J.A., et al. 2004, *AJ*, submitted

Kearns, K.M., & Herbst, W. 1998, *AJ*, 116, 261

Larwood, J.D., & Papaloizou, J.C.B. 1997, *MNRAS*, 285, 288

Larwood, J.D. 1998, *MNRAS*, 299, L32

Lubow, S.H., & Ogilvie, G.I. 2000, *ApJ*, 538, 326

Lubow, S.H., & Ogilvie, G.I. 2001, *ApJ*, 560, 997

Papaloizou, J.C.B., & Lin, D.N.C. 1995, *ApJ*, 438, 841

Papaloizou, J.C.B., & Pringle, J.E. 1983, *MNRAS*, 202, 1181

Sung, H., Bessel, M.S., & Lee, S.-W. 1997, *AJ*, 114, 2644

Terquem, C., Eisloffel, J., Papaloizou, J.C.B., & Nelson, R.P. 1999, *ApJ*, 512, L131

Weinberger, A.J., et al. 2002, *ApJ*, 566, 409

Winn, J.N., Garnavich, P.M., Stanek, K.Z., & Sasselov, D.D. 2003, *ApJ*, 593, L121

Youdin, A.N., & Shu, F.H. 2002, ApJ, 580, 494

Youdin, A.N., & Chiang, E.I. 2004, ApJ, in press, astro-ph/0309247